Journal of Low Temperature Physics (2023) 213:317–326
https://doi.org/10.1007/s10909-023-03005-w

BICEP Array: 150 GHz Detector Module Development

Alessandro Schillaci · P. A. R. Ade · Z. Ahmed · M. Amiri · D. Barkats · R. Basu Thakur, et al. ***[full author details at the end of the article]***

Received: 14 August 2023 / Accepted: 19 September 2023 / Published online: 12 October 2023

Abstract

The Background Imaging of Cosmic Extragalactic Polarization (BICEP)/Keck (BK) collaboration is currently leading the quest for the highest-sensitivity measurements of the polarized cosmic microwave background (CMB) anisotropies on a degree scale with a series of cryogenic telescopes, of which BICEP Array (BA) is the latest Stage-3 upgrade with a total of ∼ 32,000 detectors. The instrument comprises 4 receivers spanning 30–270 GHz, with the low-frequency 30/40 GHz deployed to the South Pole Station in late 2019. The full complement of receivers is forecast to set the most stringent constraints on the tensor-to-scalar ratio r. Building on these advances, the overarching small-aperture telescope concept is already being used as the reference for further Stage-4 experiment design. This paper describes the development of the BICEP Array 150 GHz detector module and its fabrication requirements, with highlights on the high-density time division multiplexing (TDM) design of the cryogenic circuit boards. The low-impedance wiring required between the detectors and the first stage of superconducting quantum interference device amplifiers is crucial to maintaining a stable bias current on the detectors. A novel multilayer FR4 Printed Circuit Board with superconducting traces, capable of reading out up to 648 detectors, is detailed along with its validation tests. An ultra-high-density TDM detector module concept we developed for a CMB-S4-like experiment that allows up to 1920 detectors to be read out is also presented. TDM has been chosen as the detector readout technology for the Cosmic Microwave Background Stage-4 (CMB-S4) experiment based on its proven low-noise performance, predictable costs, and overall maturity of the architecture. The heritage for TDM is rooted in mm- and sub-mm-wave experiments dating back 20 years and has since evolved to support a multiplexing factor of 64x in Stage-3 experiments.

Keywords Cosmology · B-mode polarization · Cosmic microwave background · BICEP array · Time division multiplexing · Transition edge sensor

1 Introduction

The search for inflationary primordial gravitational waves in the CMB polarized signal is pushing the development of larger arrays of detectors. The Stage-3 class receivers currently being deployed in Antarctica and Chile are reaching the current limits of the Time Division Multiplexing (TDM) readout capabilities. The recent outstanding results from the BICEP/Keck collaboration [1, 2] show that improving further the sensitivity on the tensor to scalar ratio r will require the development of multi-frequency ∼10,000 detector arrays. Synchrotron and dust polarized foregrounds as well as gravitational lensing distortion are presently the dominant factors on current r constraints.

With this goal in mind the BK collaboration is currently deploying the latest of the BK Series, the BICEP Array telescope [3]. This Stage-3 experiment comprises four 0.5 m aperture telescopes working at 30/40, 95, 150 and 220/270 GHz. In the 2019–2020 Austral summer, the 30/40 GHz low-frequency receiver (BA1) [4] was successfully deployed at the Amundsen-Scott South Pole Station. The ∼ 500 detector array has already collected two years of data aiming to place a more definite constraint on the faint Synchrotron polarized foreground in a 600 $\deg^2$ observing sky field. Two refurbishments have taken place in the 2021–2022 and 2022–2023 Austral summers with the goal of improving the BA1 receiver performances with new detector modules. In parallel the development of the three other BICEP-Array receivers has moved further in North America and the 150 GHz receiver (BA2) has been successfully deployed at the South Pole Station in the 2022–2023 Antarctic summer season with a partially complete FPU (5 modules out of 12) [5]. With close to 8000 transition edge sensors (TES) [6] when completed, the BA2 will have the highest density of detectors for the BK series ever. Section 2 of this paper will describe the general features of the receiver highlighting the innovative high-density readout PCB that has been specifically developed to achieve the wiring of this large number of detectors.

With more than a decade of successfully deployed CMB polarization B-mode instruments, the BK Collaboration is playing a leading role within the CMB community. The recently formed CMB-S4 Collaboration [7] is aiming to develop a large CMB observatory with more than a half million detectors to achieve extremely sensitive polarization measurements. The Small Aperture Telescope (SAT) baseline design is largely inspired by BK experience, where the BICEP Array is regarded as the state of the art for this class of instruments. In Sect. 3, a Detector Module Concept derived from BA2 experience will be presented. This concept design could potentially allow up to 2000 detectors routing capability on a 6" hexagonal package.

Table 1 Readout channels count for the three TDM BICEP Array receivers at 30/40, 95, and 150 GHz. BA1 30/40 GHz receiver is split into 2 sub-arrays, 6 modules at 30 GHz and 6 modules at 40 GHz. Each of these counts as a 0.5 MCE. The 43 Rows for the BA3 95 GHz Receiver will require an MCE firmware upgrade

Receiver observing band (GHz)	Detectors per module (per receiver)	Rows	Columns per module (per receiver)	MCEs per receiver
BICEP Array				
/BA1-30	32 (192)	33	2 (12)	0.5
\BA1-40	50 (300)	33	2 (12)	0.5
BA3-95	338 (4056)	43	8 (96)	3
BA2-150	648 (7776)	41	16 (192)	6

2 BICEP Array 150 GHz Receiver

The 150 GHz receiver design shares most of the hardware design with the other three receivers in the BICEP Array [8]. We use a combination of a pulse tube refrigerator and a Helium-3/Helium-4 3-stages sorption fridge [9] to achieve a 250 mK Focal Plane Unit (FPU) base temperature. The refractive f/1.55 2-lens High-Density Polyethylene (HDPE) optics are cooled to 4 K to reduce the radiative heat load on the detectors with the help of HDPE foam and alumina infrared (IR) blocker filters at the 300 K and 50 K stages of the receiver. Thermo-mechanical structure and the magnetic shielding of the receiver have been simulated (in COMSOL®/Solidworks®) to minimize the impact of systematics in the CMB data and to ease data reduction.

2.1 150 GHz Receiver Readout

The 30/40, 95, and 150 GHz receivers all share the well-known and proven TDM readout architecture [10]. The last receiver of the series, BA4 at 220/270 GHz, is being developed using a frequency division multiplexing called μ-MUX [11], due to the extremely large detector count. We also plan to include at least one module in the 220/270 GHz camera with thermal kinetic inductance detectors [12–14] as a demonstration of an alternative technology that would greatly simplify hardware integration and reduce risk by reducing the wirebond count by orders of magnitude. Each receiver will be furnished with 12 detector modules each one carrying a 6" detector tile. The three TDM receivers have been designed to use the same modular readout package repeated enough times depending on the number of detectors to be read.

The warm readout electronics are based on the Multi-Channel Electronics (MCE) developed by the University of British Columbia (UBC). Each MCE has

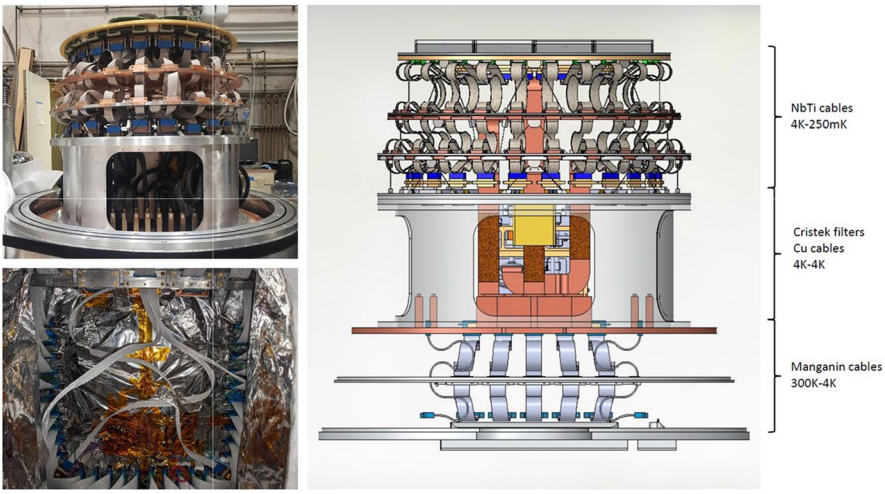

Fig. 1 *Top/Left:* 150 GHz BA2 Insert with the NbTi cables and the 4 K isothermal cables and Cristek filters. *Bottom/Left:* Bottom view of the 150 GHz BA2 300 K - 4 K Manganin cables *Bottom/Right:* 3D Model showing the full readout cable chain installed (color figure online)

32 readout channels (columns) that can be switched between 41 addresses (rows) bringing the total count to 1312 readable detectors per each of them.

In Table 1, we report the readout architecture numbers for the three TDM BICEP Array receivers. The BA2 receiver with 7776 Detectors will require 6 MCEs which presents an additional challenge of warm electronic space allocation.

The readout uses 30×100 ways manganin cables, to carry electrical signals with minimal heat load from 300 K to the 50 K and 4 K stages of the cryostat (see Fig. 1). These low thermal conductivity cables are sized to minimize the conductive heat load from 300 K to the 50 K and 4 K stages of the cryostat. Entering the 4 K cryostat volume all wiring is passed through a stage of RF low pass filters.[1] Next in the chain, simple copper iso-thermal cables connect to a stage of SQUID Series Array (SSA). A last set of 18 100-ways Niobium–Titanium (NbTi) cables (3 per MCE) is used for the last section of the readout chain for connecting the SSA modules at 4 K up to a 0.250 K distribution board at the FPU. The choice of the NbTi superconducting cable is driven by the low current signals produced by the TES detectors which require low-impedance circuitry. Also, these cables have been carefully sized to prevent unwanted conductive heat load from reaching the coldest volume of the instrument.

At the FPU, a large distribution PCB directs the signals to the 12 detector modules. The connection to this last step is made using four 60-way cryogenic Kapton-embedded copper Flat Flex cables.

[1] Cristek micro-D saver PI filtered, model no. C48-00063-01.

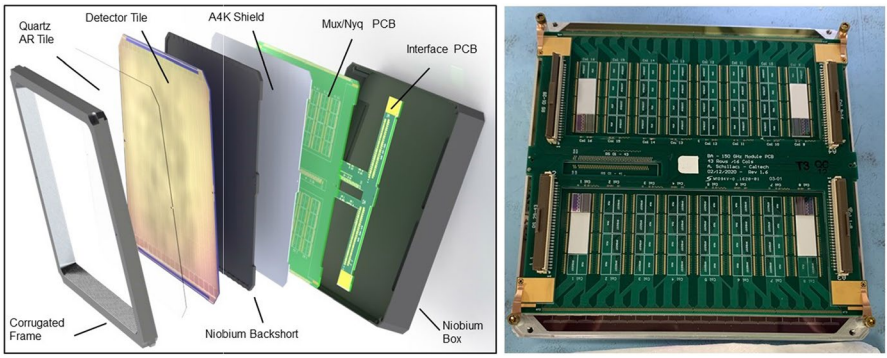

Fig. 2 *Left:* Exploded view of the 150 GHz BA2 Detector Module. *Right:* Open Test Module showing the module PCBs. Only 4 pairs of MUX/Nyq Chips are mounted (on ceramic carriers) for the purpose of the superconductivity test. The testing detector tile can be seen at the top and bottom edges of the PCB. (color figure online)

2.2 150 GHz Module

The main architecture of the detector modules is shared among the 3 TDM receivers (Fig. 2). The relevant opto-mechanical differences are driven by the different frequencies assigned to a module. The frequency band of the receiver determines the design and optimization of the module $\lambda/4$ backshort, the quartz anti-reflection coating tile, and the corrugated frames [15]. All of the BA detector modules have a high-performance magnetic shield in the form of a niobium box plus an inner sheet of A4K high magnetic permeability steel for protecting the multiplexing chips carrying the SQUIDS (for a detailed description of the magnetic shielding see [3]). These are National Institute of Standards and Technology (NIST) Nyquist (Nyq) and multiplexing (MUX) chips [16, 17] and they are glued and wirebonded on aluminum nitride substrate with aluminum traces single layer PCBs. This PCB provides the routing to interface with the detector tile above it. The choice of superconductive traces (aluminum critical temperature is around 1 K) is driven by the necessity to have low-resistance circuitry between the detectors and the SQUIDs to keep the detector stable [18]. The low resistance of the TES detectors when in operation (a few milliohms) needs to be well matched with very low impedance wiring, generally less of the shunt resistor used in the circuit (in our case about 3 milliohms).

This choice worked flawlessly with the low-frequency receiver BA1 but the large number of traces that will need to be connected for BA2 required the development of a new FR4 multi-layer PCB. We found trying to achieve this density with a commercial single-layer PCB was costly and low yield.

Comparing the commercial prices for aluminum nitride single-layer and multi-layer FR4 PCBs, the former can cost up to $\$5,000$ per board, while the latter is about 20 times cheaper ($250 each).

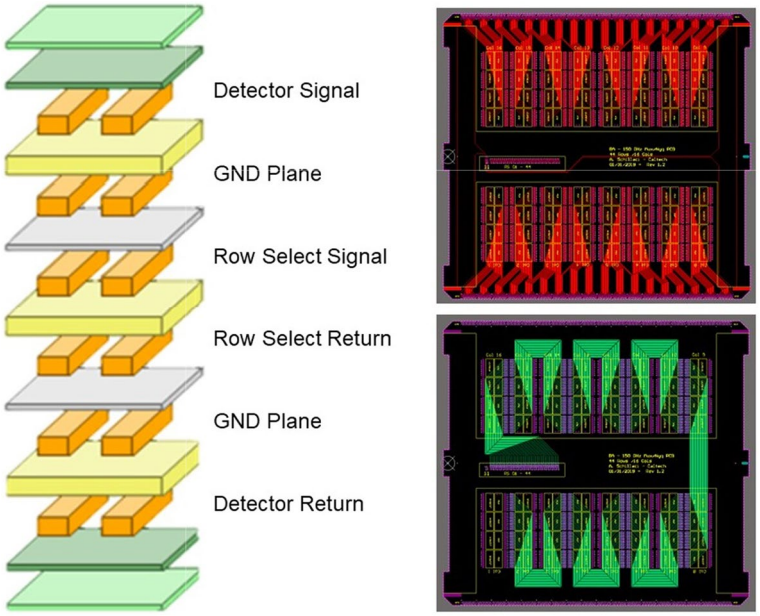

Fig. 3 *Left:* Exploded view of the layer stack for the 150 GHz MUX/Nyq PCB. The top and bottom layers are the ones that go to the detectors and that need the tin/lead plating for achieving superconductivity *Right/Top:* 150 GHz MUX/Nyq PCB top layer with superconductive traces carrying the detector signals (detector returns are similarly routed on the bottom layer) *Right/Bottom:* 150 GHz MUX/Nyq PCB middle layer with normal conductive traces carrying the row select signals (the row select returns are similarly routed on a second middle layer). All these figures have been produced using ALTIUM® software. (color figure online)

2.3 150 GHz MUX/Nyq Interface PCB Superconductivity Test

Referring to Fig. 3, the 150 GHz MUX/Nyq PCB is a compact and high trace density 6-layer FR4 design. Traces have a copper weight of 0.5 oz (equivalent to 0.0175 mm thickness) with a width/pitch of 3/6 mil (76/152 micron). Two middle layers have been used for the row select routing and have been packed in between 2 ground planes in order to minimize the cross-talk. The outer top and bottom layers have been used for the detector wiring that requires superconductive traces. To achieve that, we asked the manufacturer (TTM Technologies, North Jackson[2]) to plate the copper traces with a tin/lead unfused plating with a minimum thickness of 100 micro-inches (2.54 microns). After manufacturing the achieved thickness has been measured by TTM to have an average value of 400 micro-inches, which is comfortably above our minimum requirement.

Before assembling a fully chip-populated 150 GHz module (each unit requires 64× MUX and 64 Nyquist Chips), we performed a test on the top and bottom Sn/

[2] https://www.ttm.com/

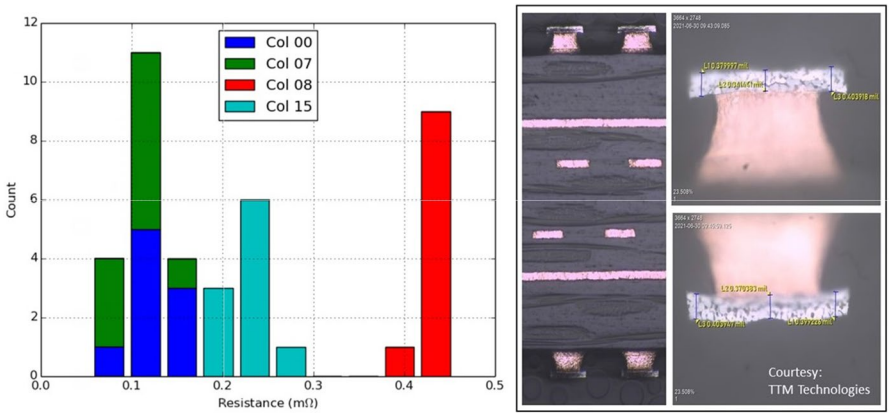

Fig. 4 *Left:* Resistance measurements histogram on the 40 channels we tested in the MUX/Nyq PCB. Colors and labels specify the sub-set (column) of channels grouped on the same readout chips. *Right:* Pictures of one sliced 150 GHz MUX/Nyq PCB showing the layer stack. In the zoom panels, the Top and Bottom traces of Sn/Pb unfused plating are shown and its thickness is measured at about 400 micro-inches. Pictures courtesy TTM Technologies, North Jackson. (color figure online)

Pb plated traces of this PCB aimed to verify traces superconductivity. This test unit with just 4 chip pairs is shown in the right panel of Fig. 2. It was tested in a 0.25 K test-bed cryostat at Caltech. We tested a sample of 40 channels within the 648 available. The channels were distributed in 4 groups of 10, one group per quadrant of the PCB in order to monitor the uniformity of the Sn/Pb plating. The channels were terminated with a niobium superconducting short deposited on the test silicon wafer in place of the TES detector. In this way, we could avoid any additional in-series contribution that could affect our measurements. The trace resistance is measured by sweeping I_{bias} and measuring I_{tes} with the MCE readout electronics and converting the slope $I_{\mathrm{tes}}/I_{\mathrm{bias}}$ to a resistance, where I_{tes} is the current through the trace and I_{bias} is the input bias current to a parallel circuit of the trace and a 3 milliohms shunt resistor. The histogram on the left panel of Fig. 4 shows that the residual resistance measured at the 40 tested channels are all below 0.5 milliohms confirming the achieved superconductivity of the traces and well below the shunt resistor value.

We have integrated these PCBs in the 150 GHz BA2 detector modules and 5 of them have been tested and deployed in Antarctica. Our plan is to test the other 7 to be deployed in the 2023–2024 Austral summer to complete the BA2 receiver FPU with a total of 12 units.

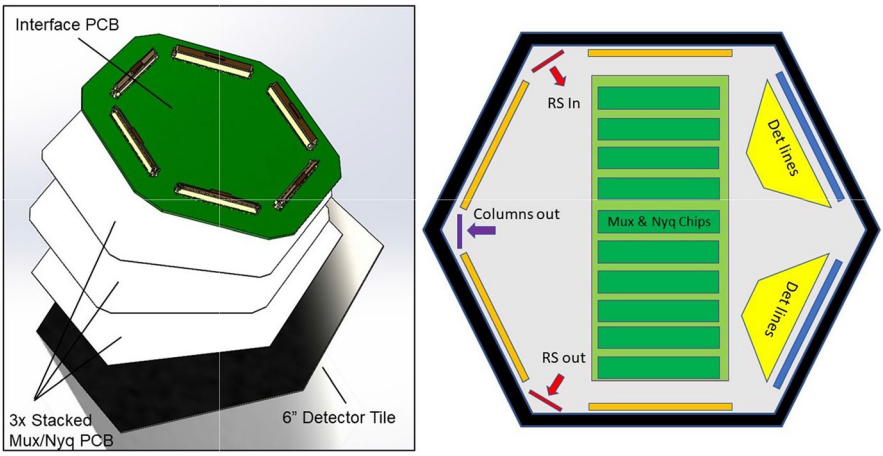

Fig. 5 *Left:* 3D exploded model of the staked multi-layer PCB design. The interface PCB and the 6" detector tile are shown in the stack. *Right:* Concept diagram of the single MUX/Nyq PCB showing the location of the wirebond pad groups at the edges. Each PCB will serve two sides of the hexagon. Also, the column and row select wirebond pad groups buses that will route between the 3 PCBs are shown. (color figure online)

3 CMB Stage-4 High Density Detector Module Concept

CMB Stage-4 is meant to deploy ~500,000 TES Detectors in the next decade between the South Pole and the Atacama Desert. These large number of new telescopes will range between 20 GHz and 270 GHz. The highest frequency modules will approach 2000 TES Detectors on a hexagonal 6" tile, making the design of a MUX/Nyq PCB very challenging.

In Fig. 5, a readout concept design with 3 multi-layer MUX/Nyq PCB stacked and interconnecting wirebond buses is illustrated. With 64 rows and 30 columns distributed within the 3 stacked PCBs, the design could potentially achieve the required large wiring capability of the next generation Stage-4 high-frequency receiver modules.

On this framework, the experience with the development of the BICEP Array MUX/Nyq PCB described in this paper can be a valuable reference for the next-generation TDM instrument readout.

Acknowledgements The BICEP/Keck project has been made possible through a series of grants from the National Science Foundation including 0742818, 0742592, 1044978, 1110087, 1145172, 1145143, 1145248, 1639040, 1638957, 1638978, 1638970, & 1726917 and by the Keck Foundation. The development of antenna-coupled detector technology was supported by the JPL Research and Technology Development Fund and NASA Grants 06-ARPA206-0040, 10-SAT10-0017, 12-SAT12-0031, 14-SAT14-0009 & 16-SAT16-0002. The development and testing of focal planes were supported by the Gordon and Betty Moore Foundation at Caltech. Readout electronics were supported by a Canada Foundation for Innovation grant to UBC. The computations in this paper were run on the Odyssey cluster supported by the FAS Science Division Research Computing Group at Harvard University. The analysis effort at Stanford and SLAC is partially supported by the U.S. DoE Office of Science. We thank the staff of the U.S. Antarctic Program and in particular, the South Pole Station without whose help this research would not have been

possible. Tireless administrative support was provided by Kathy Deniston, Sheri Stoll, Nancy Roth-Rappard, Irene Coyle, Donna Hernandez, and Dana Volponi.

References

1. Bicep/Keck Collaboration Phys, Rev. Lett. **127**, 15 (2021). https://doi.org/10.1103/PhysRevLett.127.151301
2. Bicep/Keck Collaboration Phys, Rev. Lett. **121**, 22 (2018). https://doi.org/10.1103/PhysRevLett.121.221301
3. L. Moncelsi et al., Proc. SPIE **11453**, 1145314 (2020). https://doi.org/10.1117/12.2561995
4. A. Schillaci et al., J. Low Temp. Phys. (2020). https://doi.org/10.1007/s10909-020-02394-6
5. S. Fatigoni, et al, *J. Low Temp. Phys. Proceeding of LTD20*, **In preparation** (2023)
6. BICEP2 Collaboration *APJ*, **812**, issue 2, (2015), https://doi.org/10.1088/0004-637X/812/2/176
7. CMB-S4 Collaboration *eprint on ArXiv* eprint arXiv:1907.04473 (2019)
8. M. Crumrine et al., Proc. SPIE (2018). https://doi.org/10.1117/12.2312829
9. L. Duband *eprint on ArXiv* eprint arXiv:2009.09997 (2020)
10. E.S. Battistelli et al., J. Low Temp. Phys. (2008). https://doi.org/10.1007/s10909-008-9772-z
11. A. Cukierman et al., J. Low Temp. Phys. (2020). https://doi.org/10.1007/s10909-019-02296-2
12. A. Wandui et al., JAP **128**(4), 044508 (2020). https://doi.org/10.1063/5.0002413
13. L. Minutolo et al., Proc. IEEE **31**(5), 3069732 (2021). https://doi.org/10.1109/TASC.2021.3069732
14. A. Wandui et al., Proc. SPIE **11453**, 114531E (2020). https://doi.org/10.1117/12.2563373
15. A. Soliman et al., Proc. SPIE **10708**, 107082G (2018). https://doi.org/10.1117/12.2312942
16. P.A.J. de Korte et al., Rev. Sci. Inst. **74**, 3807 (2003). https://doi.org/10.1016/j.nima.2003.11.310
17. K.D. Irwin et al., J. Low Temp. Phys. (2012). https://doi.org/10.1007/s10909-012-0586-7
18. K.D. Irwin et al., Appl. Phys. (2005). https://doi.org/10.1007/10933596-3

Authors and Affiliations

Alessandro Schillaci[1] · P. A. R. Ade[2] · Z. Ahmed[3,4] · M. Amiri[5] · D. Barkats[6] · R. Basu Thakur[1] · C. A. Bischoff[7] · D. Beck[4] · J. J. Bock[1,8] · V. Buza[6] · J. Cheshire[9] · J. Connors[6] · J. Cornelison[6] · M. Crumrine[9] · A. Cukierman[4] · E. Denison[13] · M. Dierickx[6] · L. Duband[10] · M. Eiben[6] · S. Fatigoni[5] · J. P. Filippini[11,12] · C. Giannakopoulos[7] · N. Goeckner-Wald[4] · D. Goldfinger[6] · J. A. Grayson[4] · P. Grimes[6] · G. Hall[9] · G. Halal[4] · M. Halpern[5] · E. Hand[7] · S. Harrison[6] · S. Henderson[3,4] · S. R. Hildebrandt[8] · G. C. Hilton[13] · J. Hubmayr[13] · H. Hui[1] · K. D. Irwin[3,4] · J. Kang[4] · K. S. Karkare[6,14] · S. Kefeli[1] · J. M. Kovac[6] · C. L. Kuo[3,4] · K. Lau[1] · E. M. Leitch[14] · A. Lennox[11] · K. G. Megerian[8] · O. Y. Miller[1] · L. Minutolo[1] · L. Moncelsi[1] · Y. Nakato[4] · T. Namikawa[15] · H. T. Nguyen[8] · R. O'Brient[1,8] · S. Palladino[7] · M. Petroff[6] · N. Precup[9] · T. Prouve[10] · C. Pryke[9] · B. Racine[6] · C. D. Reintsema[13] · B. L. Schmitt[6] · B. Singari[9] · A. Soliman[1] · T. St. Germaine[6] · B. Steinbach[1] · R. V. Sudiwala[2] · K. L. Thompson[3,4] ·

C. Tucker[2] · A. D. Turner[8] · C. Umiltà[7] · C. Verges[6] · A. G. Vieregg[14] · A. Wandui[1] · A. C. Weber[8] · D. V. Wiebe[5] · J. Willmert[9] · W. L. K. Wu[14] · E. Yang[4] · K. W. Yoon[4] · E. Young[4] · C. Yu[4] · L. Zeng[6] · C. Zhang[1] · S. Zhang[1]

✉ Alessandro Schillaci
aleschillaci78@gmail.com

[1] Department of Physics, California Institute of Technology, Pasadena, CA 91125, USA

[2] School of Physics and Astronomy, Cardiff University, Cardiff CF24 3AA, UK

[3] SLAC National Accelerator Laboratory, Kavli Institute for Particle Astrophysics and Cosmology, 2575 Sand Hill Rd, Menlo Park, CA 94025, USA

[4] Department of Physics, Stanford University, Stanford, CA 94305, USA

[5] Department of Physics and Astronomy, University of British Columbia, Vancouver, BC V6T 1Z1, Canada

[6] Harvard-Smithsonian Center for Astrophysics, Cambridge, MA 02138, USA

[7] Department of Physics, University of Cincinnati, Cincinnati, OH 45221, USA

[8] Jet Propulsion Laboratory, Pasadena, CA 91109, USA

[9] Minnesota Institute for Astrophysics, University of Minnesota, Minneapolis 55455, USA

[10] Service des Basses Températures, Commissariat à lEnergie Atomique, 38054 Grenoble, France

[11] Department of Physics, University of Illinois at Urbana-Champaign, Urbana, IL 61801, USA

[12] Department of Astronomy, University of Illinois at Urbana-Champaign, Urbana, IL 61801, USA

[13] National Institute of Standards and Technology, Boulder, CO 80305, USA

[14] Kavli Institute for Cosmological Physics, University of Chicago, Chicago, IL 60637, USA

[15] Department of Applied Mathematics and Theoretical Physics, University of Cambridge, Wilberforce Road, Cambridge CB3 0WA, UK